Evidence for an actin binding helix in gelsolin segment 2; have homologous sequences in segments 1 and 2 of gelsolin evolved to divergent actin binding functions?

M. Van Troys, D. Dewitte, M. Goethals, J. Vandekerckhove, C. Ampe*

Flanders Interuniversity Institute for Biotechnology, Department of Biochemistry, Faculty of Medicine, Universiteit Gent, Ledeganckstraat 35, 9000 Ghent, Belgium

Received 6 September 1996

Abstract Gelsolin is built up of six homologous segments that perform different functions on actin. Segments 1 and 2, which are suggested to be highly similar in their overall folds, bind monomeric and filamentous actin respectively. A long α-helix in segment 1 forms the major contact site of this segment with actin. We show that sequence 197–226 of segment 2, equivalent to the region around the actin binding helix in segment 1, contains F-actin binding activity. Consequently, positionally similar parts of segment 1 and 2 are implicated in the actin contact and solvent exposed residues in these parts must have evolved differentially to meet their different actin binding properties.

Key words: Crosslinking; F-actin binding; Gelsolin; Peptide mimetic

1. Introduction

Gelsolin is a 83 kDa actin binding protein, ubiquitously present in vertebrates, both in the cytoplasm and in extracellular fluids [1]. It is probably the most versatile actin modulating protein; in vitro it binds actin monomers, promotes nucleation, binds filaments, breaks them and shields their fast-growing ends. This actin binding activity is regulated by Ca^{2+} and phosphoinositides, pointing at a key role for gelsolin in signal transduction and microfilament rearrangements [2]. It belongs to a superfamily of actin binding proteins (additionally containing villin, severin, fragmin and others) and has evolved from a small unit of approximately 15 kDa ([3] and references therein). Gelsolin consists of six such repeats whose functions in actin binding were characterized using limited proteolysis and recombinant techniques [4–6]. Both segment 1 (S1, residues 1–149 in human gelsolin (HGS)) and segments 4–6 (S4–6, residues 407–755 in HGS) bind actin monomers. Pope et al. [7] showed that actin binding by the COOH-terminal half of gelsolin is restricted to S4, while S5 and S6 are involved in Ca^{2+} regulation. S1 and S4 bind to a similar site on the actin molecule [8] and their simultaneous binding to two monomers underlies the nucleation promoting property of gelsolin. Segments 2–3 (S2–3, residues 150–406 in HGS) form the F-actin binding part and this binding is Ca^{2+}-independent and stoichiometric. Deletion analysis limited the filament binding site to S2 [9].

Filament severing and capping have been proposed to occur in two consecutive steps. First, S2 binds to the side of the filament and positions S1, which in its turn disrupts actin-actin contacts. S1 stays strongly bound to the newly made barbed end and prevents both dissociation and association of actin monomers. Experimental evidence underlies this model. Way et al. [10] demonstrated that a chimera of gelsolin S1 and the α-actinin F-actin binding unit forms a functional filament severing and capping protein. Yu et al. [11] showed that gCap39, a gelsolin homologue that caps but does not sever filaments, gains the severing function when S1 of gCap39 was linked to S2–3 of gelsolin, indicating that the F-actin side-binding (by S2) is a prerequisite for efficient severing. Consequently, the effect on severing is often used as an assay because of the necessity of F-actin binding for this activity.

Recently, structural data, both of isolated segments and of segments in complex with monomeric actin, have emerged elucidating actin binding at the molecular level [12–14]. Gelsolin S1 binds in the cleft between actin subdomains 1 and 3 and contacts them through a long α-helix (residues 95–112 in HGS) located near the end of segment 1. NMR analysis revealed that S2 of severin has a highly similar fold to S1 of gelsolin and villin.

While the actin interacting residues in S1 have been clearly defined, the filament binding sequence of S2 is not yet known in detail. Several studies, analyzing either COOH-terminal extension of S1 [7,15] or NH_2-terminal shortening of S2 [16], suggest that the NH_2-terminus of S2 (residues 150–173) is involved. A synthetic villin peptide (residues 133–147, corresponding to gelsolin residues 159–171) binds to actin and mutation of basic residues in this sequence affects severing [17]. However, several observations suggest that still other residues of segment 2 are involved in F-actin side-binding. The severing activity of recombinant gelsolin (1–160) or severin (1–177) fragments containing only small portions of S2 (11 and 26 residues of S2, respectively) is marginal compared to the maximal activity. In contrast, severin 1–277, containing S1 and the entire S2 domain, has full severing activity [15]. The capping protein gCap39 gained severing function by replacing sequences in the actin binding helix of S1 and in the NH_2-terminus of S2 with the respective gelsolin sequences, but again maximal activity was not attained [18].

In this study we demonstrate that the more COOH-terminal part of S2 also contributes to F-actin binding. We show that a synthetic peptide containing the sequence of human gelsolin segment 2, homologous to the actin binding helix of segment

*Corresponding author. Fax: (32) (9) 264 53 37.

Abbreviations: EDC, 1-ethyl-3(3-dimethylaminopropyl)carbodiimide; CD, circular dichroism; HGS, human gelsolin; PS1, peptide (residues 88–117) from gelsolin segment 1; PS2, peptide (residues 197–226) from gelsolin segment 2; TFE, 3,3,3-trifluoroethanol

PII S0014-5793(96)01086-1

1, binds to F-actin and competes with gelsolin segment S2–3. This indicates that the filament binding sequence in gelsolin S2 is more extensive than previously thought and suggests that within a structurally similar framework different actin binding sites have evolved.

2. Materials and methods

2.1. Proteins and peptides

We prepared rabbit skeletal muscle actin following the procedure of Spudich and Watt [19] and isolated it as Ca-G-actin by chromatography over Sephadex G-200 in G-buffer (5 mM Tris-HCl pH 7.7, 0.1 mM $CaCl_2$, 0.2 mM ATP, 0.2 mM DTT, 0.01% NaN_3). Pyrene-labelled actin was prepared as in [20]. We chemically synthesized the gelsolin peptides (PS2 and PS1) on a model 431A peptide synthesizer (Applied Biosystems Inc., Foster City, CA). They were purified as in [21], checked for correct mass by matrix-assisted laser desorption ionization time of flight mass spectroscopy and their concentration was determined as in [21]. The PS2 peptide we used carries an NH_2-terminal cysteine residue, while the internal cysteine (residue 202) is replaced by serine. In some experiments we labelled this cysteine with *N*-pyrenyliodoacetamide (Molecular Probes) by adding the label in a threefold molar excess to the peptide in 100 mM Tris-HCl pH 8.8. The reaction was kept at room temperature overnight and quenched with DTT. We prepared human plasma gelsolin and digested it with α-chymotrypsin following the procedure in [5]. The gelsolin fragments were further purified and their concentration determined as in [5]. NH_2-terminal sequence analysis was performed on a 470A Sequenator equipped with an on-line 120A phenylthiohydantoin amino acid analyzer (Applied Biosystems Inc.).

2.2. Actin binding assays and competition assays

2.2.1. Via chemical crosslinking. A G-actin solution was dialysed overnight against phosphate buffer (5 mM K-phosphate pH 7.5, 0.2 mM $CaCl_2$, 0.2 mM ATP, 0.2 mM DTT). As binding to F-actin was under study, we induced polymerization by adding KCl and $MgCl_2$ (respectively 100 mM and 1 mM final concentrations) followed by 20 min incubation at room temperature. We added the peptide in various molar ratios to these preformed actin filaments (final concentration 3 μM) and incubated them for 1 h at room temperature. Then the zero-length crosslinker 1-ethyl-3(3-dimethylaminopropyl)carbodiimide (EDC) (Sigma) and *N*-hydroxy-sulfosuccinimide (Pierce) were added to a final concentration of 4 mM [22]. The reaction was kept at room temperature for another 45 min. We analyzed aliquots of the samples on SDS-PAGE mini slab gels which were stained with Coomassie.

Due to the relatively low concentration of the S2–3 fragment, we performed all crosslinking experiments at an F-actin concentration of 3 μM and incubation times were extended to 1 h at room temperature, followed by overnight incubation at 4°C. The S2–3 concentrations used are indicated in the figure legends. To assay for competitive binding of S2–3 and PS2 using chemical crosslinking, we first added a constant amount of PS2 30 μM to a series of samples containing 3 μM F-actin. After incubation to allow complex formation, we added increasing concentrations of S2–3 and again incubated the samples. At this point, crosslinker was added and the further procedure was as described above. To further demonstrate the peptides' interaction with F-actin protomers, we combined chemical crosslinking with sedimentation. The samples containing actin in the presence or absence of PS2 in polymerizing buffer, incubated with the crosslinker as outlined above, were spun at $100\,000 \times g$ in a Beckman airfuge for 20 min at room temperature. Supernatants and resuspended pellets were analyzed on SDS-mini slab gels followed by Coomassie staining.

2.2.2. Via fluorometric measurements. We added the peptide in increasing concentration (0–180 μM, 10% labelled) to a series of samples containing 4 μM F-actin and allowed them to interact overnight at room temperature to ensure equilibrium was reached. A series containing only peptide was also prepared. The measured fluorescence of this series was subtracted from the fluorescence of the samples containing F-actin, which resulted in a nett fluorescence. This nett relative steady-state fluorescence was plotted against the total concentration of peptide. We calculated a K_d for the peptide–F-actin interaction using the equation

$$1/AP^* = K_d/[P_t A_t(1/1 + k)] + 1/[A_t(1/1 + k)]$$

with A_t and P_t the total concentrations of F-actin and peptide (labelled+non-labelled) respectively. AP^* is the equilibrium concentration of the complex of F-actin subunits with labelled peptide and k the ratio of non-labelled over labelled peptide. This equation is derived from the one for the equilibrium dissociation constant (K_d) of the peptide–actin complex, assuming (i) that the affinity of labelled and non-labelled peptide for F-actin is the same and (ii) that at the molar ratios in the experiment, the amount of free peptide equals the total amount of peptide, i.e. the amount of bound peptide is negligible. To meet this last requirement, we only used data points in which the molar ratio of peptide versus actin was higher than 40. In this assay the measured relative fluorescence is directly proportional to AP^*. By plotting 1/fluorescence versus $1/P_t$ we derived the K_d from the point of intersection with the X-axis (at $Y = 0$, $X = -1/K_d$).

We also tested the competitive character of PS2 and S2–3 using a severing assay. In this assay actin filaments (12 μM, 25% pyrene labelled) that are precapped at their barbed end by gelsolin (50 nM) are diluted to 0.4 μM in G-buffer. The rate of depolymerization is proportional to the concentration of pointed filament ends and consequently increases when additional gelsolin is added and exerts its severing activity on F-actin especially when the sample is simultaneously diluted below the critical monomer concentration of the pointed end (final gelsolin concentration is 50 nM). We performed this assay after incubation of the filaments for 20 min at room temperature with 100 μM PS2 (or buffer for control samples) prior to diluting to 0.4 μM F-actin.

2.3. Circular dichroism (CD) measurements

We performed CD measurements at pH 7.5 and 20°C, scanning from 184 to 260 nm, on a Jasco 600 spectropolarimeter with a step resolution of 0.5 nm and at a peptide concentration of 40 μM. 3,3,3-Trifluoroethanol (TFE) was added to a final concentration of 60%. The data are the average of nine scans and are expressed as θ_{MRW} (mean residue weight ellipticity) as a function of wavelength.

2.4. Immunoassays

The rabbit polyclonal anti-actin antibodies against part of subdomain 4 or against the COOH-terminus were produced by the Centre d'Economie rurale, Laboratoire d'hormonologie (Marloie, Belgium). Chemically synthesized actin peptides (residues 228–257 and 354–375) coupled to keyhole limpid hemocyanin, following the procedure of Mumby and Gilman [23], were used as antigen. The monoclonal α-sarcomeric actin specific antibody was obtained from Sigma. Western blots of F-actin–S2–3 and F-actin–PS2 were performed as described in [24].

3. Results

3.1. Residues 198–227 of gelsolin segment 2 are implicated in F-actin binding

The major interaction site of gelsolin S1 with actin is formed by an α-helix located in the COOH-terminal part of this segment [12]. Structural proof exists that segments 1 and 2 adopt a similar fold [13], which suggests a functional similarity in their contact with actin. This urged us to analyze the properties of the synthetic peptide covering the S2 region homologous to the actin binding helix of S1. The peptide spans S2 residues 198–227 (PS2, Fig. 1).

We first employed the zero-length crosslinker EDC, which covalently couples COOH and NH_2 groups in close proximity at the contact sites, to probe binding of the peptide to F-actin. Fig. 2a shows that PS2 crosslinks, ergo binds, efficiently to actin under polymerization conditions. At an F-actin protomer concentration of 3 μM, 30 μM of peptide resulted in 50% crosslinked actin–peptide complex. Spinning this sample at high speed revealed that the peptide actually associates with actin protomers in the preformed fila-

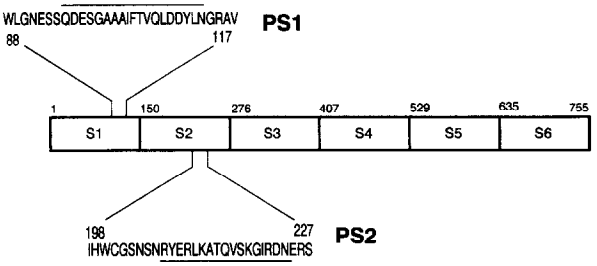

Fig. 1. Segmental structure of human gelsolin. The positions of the peptides PS1 and PS2 are shown as well as the position of the actin binding α-helix within these sequences (underlined). The α-helical portion of the PS2 sequence is based on the sequence alignment with severin domain 2 [13].

ments, as the crosslinked actin–PS2 complex cosedimented (Fig. 2b).

We synthesized PS2 with a cysteine at its extreme NH_2-terminus enabling it to be labelled with the fluorophore *N*-pyrenyliodoacetamide. Adding this labelled peptide to polymerized actin in F-buffer results in a rise in fluorescence (Fig. 2c), most likely due to a change in the environment of the attached fluorophore upon formation of the peptide–actin complex. Using an actin concentration of 4 μM, a concentration of ca. 180 μM of peptide proved to be sufficient to obtain a nearly plateau value in fluorescence. From this curve we determined (see Section 2 and inset Fig. 2c) an equilibrium dissociation constant for the F-actin protomer–PS2 complex of ca. 125 μM, note that this is on the assumption that labelled and non-labelled peptide bind with the same affinity.

3.2. The S2 peptide adopts a similar conformation as the S1 peptide

Using circular dichroism as a measure for secondary structure, we demonstrate that the peptide 198–227 does not adopt a stable or unique conformation in aqueous solution at room temperature. However, adding 60% TFE renders a CD spectrum typical for an α-helix with a maximum at 190 nm and a double minimum at 208 and 222 nm (Fig. 3). Fluorinated alcohols are known to propagate α-helices by stabilizing internal H-bridge formation, but do so only when a helix-forming propensity is present [25]. A synthetic peptide (S1 residues 88–117) containing the S1 actin binding helix shows a similar behavior as the S2 peptide, i.e. random coil in aqueous solution and α-helical (as it is in its protein environment [12]) in 60% TFE (Fig. 3).

3.3. The S2 peptide (PS2) competes with segment 2+3 (residues 150–407) for binding to F-actin

As was shown in earlier studies, the α-chymotryptically obtained fragment consisting of gelsolin segments 2 and 3 binds to actin filaments. By NH_2-terminal sequence analysis we confirmed that the S2–3 we used here starts at segment 2 residue 150. Adding increasing amounts of S2–3 to F-actin (3 μM) preincubated with PS2 (total concentration 30 μM) results in a decrease of actin–peptide crosslink concomitant with the appearance of the S2–3 actin crosslink (Fig. 4). The yield of S2–3 crosslinking to F-actin as a function of total added S2–3 is significantly lower when S2–3 was added to preformed filaments that were first saturated with the PS2 than in its absence, indicating that S2–3 has to displace PS2 prior to binding.

3.4. Filament severing by gelsolin is slower in the presence of PS2

We tested the severing activity of human plasma gelsolin in the absence and presence of PS2 using a dilution assay. We incubated precapped filaments with PS2 in concentrations at which, considering the determined K_d value for the actin–PS2 complex, all F-actin should be complexed. We next diluted the sample 12-fold to final actin and PS2 concentrations of 0.4 and 100 μM, respectively. Fig. 5 shows the rate of depolymerization as a function of time. Interestingly, adding the peptide to pyrenylated F-actin results in a higher fluorescence suggesting that the environment of the fluorophore changes upon

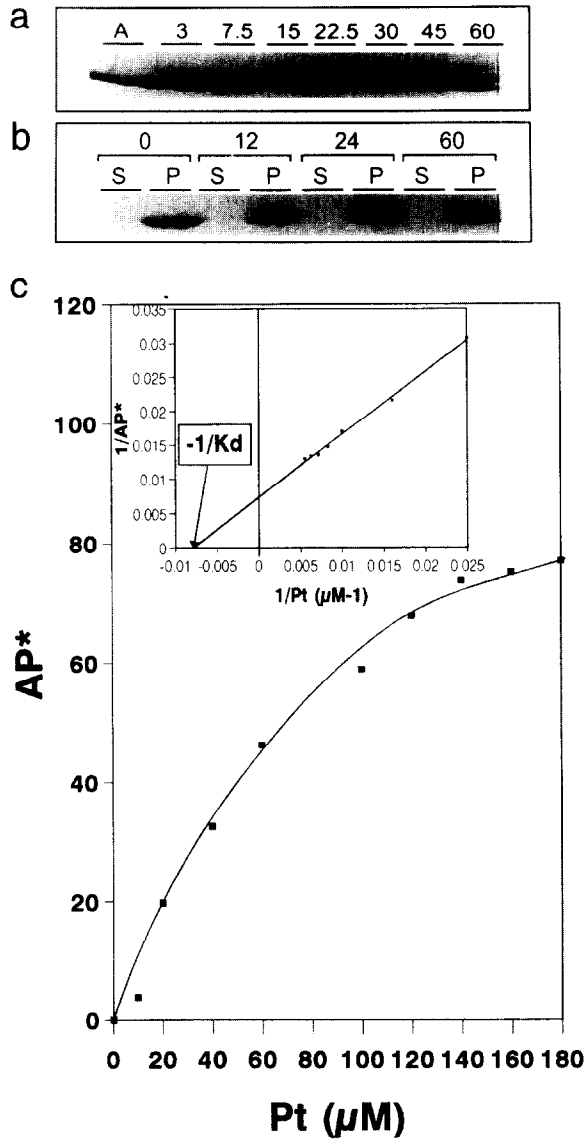

Fig. 2. Actin binding activity of the gelsolin segment 2 peptide PS2. (a) SDS analysis of EDC crosslinking between prepolymerized actin and PS2. The total actin concentration is 3 μM, the concentration of PS2 is indicated in μM above each lane. (b) SDS analysis of pellets (P) and supernatants (S) obtained after sedimentation of a EDC crosslinking reaction of 12 μM of F-actin with PS2 at the indicated concentration (μM). (c) The net relative fluorescence (%) is shown in function of total PS2 concentration of a series of samples containing 4 μM of F-actin and varying amounts of PS2 of which 10% NH_2-terminally carries the fluorophore pyrene. Inset: Determination of K_d value for PS2 binding to F-actin (see Section 2).

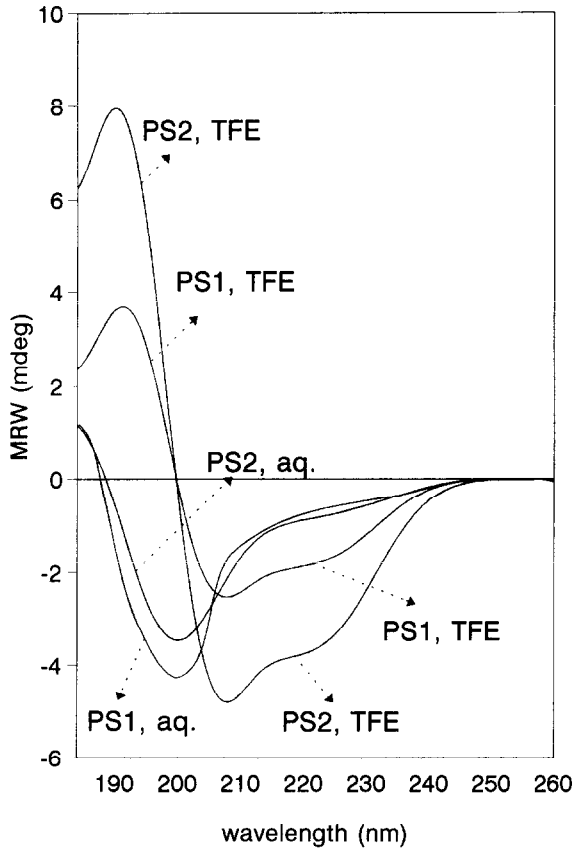

Fig. 3. Circular dichroism measurements of PS2 and PS1. Mean residue weight elipticity θ_{MRW} is shown as a function of wavelength. Curves carrying the indications 'aq.' and 'TFE' result from measuring in 10 mM Na-phosphate pH 7.5 and 60% TFE in Na-phosphate, respectively.

binding of PS2 to F-actin. Adding gelsolin to this sample does not result in a decrease of the fluorescence which accompanies severing activity (compare the difference between the upper two curves with the one between the lower two curves in Fig. 5), indicating that the severing activity is considerably slowed down when PS2 is bound to the filament.

3.5. Limiting the target site of PS2 in actin

The F-actin–PS2 and F-actin–S2–3 crosslinked complexes were screened for recognition by a set of site-specific anti-actin antibodies. We used three antibodies recognizing different epitopes in actin. One specifically recognizes actin residues 354–375 (extreme COOH-terminus) and another residues 228–257 in actin subdomain 4. A third commercial antibody is specific for α-sarcomeric actin and we determined that its epitope lies between residues 12 and 44 (part of subdomains 1 and 2) (unpublished results). When the antibody fails to recognize the crosslinked complex, this suggests that the crosslinked partner is blocking its epitope on actin. This approach is validated by the failure of the antibody, raised against the COOH-terminus of actin, to recognize the actin-bovine profilin I-crosslink, as X-ray diffraction crystallography data and chemical crosslinking experiments have shown that the extreme actin COOH-terminus is involved in the actin–profilin contact [26,27]. All three antibodies recognize the F-actin–PS2 and F-actin–S2–3-complex on Western blot as efficiently as the non-crosslinked actin (Fig. 6), indicating that neither the extreme actin COOH-terminus, the top of actin subdomain 4 nor a region between actin residues 12 and 44 is located at the site of crosslinking.

4. Discussion

In this report we show that the human gelsolin S2 peptide PS2, ranging from residues 198 to 227, binds actin filaments with a K_d of ca. 125 μM, which is relatively low considering the small size of the fragment. For comparison, the affinity of the total S2–3 fragment for actin filaments has been reported to be between 0.2 and 3 μM [11]. The specificity of the PS2 interaction is additionally demonstrated by its evident competition with the total S2–3 segment for binding to F-actin. Bound to the filament, PS2 hinders S2–3 binding and in addition decelerates filament severing by intact gelsolin.

Earlier studies have pointed out the importance in F-actin binding of the first 23 residues of segment 2 in gelsolin and related proteins. A synthetic peptide from the NH_2-terminus of S2 (residues 133–147 in villin, 159–171 in gelsolin) binds to filaments [17]. These data are not necessarily in conflict with the new F-actin binding site we identified here. Truncation analysis shows that mutants containing S1 in combination with these 23 residues have severing activity, for which F-actin binding is a prerequisite. However, the severing activity is severely reduced indicating that not all binding information is present in this mutant. We hypothesize that this NH_2-terminal S2 region (150–173) and the α-helical segment we identified in the COOH-terminus (residues 198–227) cooperate to form the F-actin binding site of gelsolin and that both sequences are necessary to obtain full side-binding and severing activity. Diverse data underlie our cooperative binding model. First, S2 is presumed to bind to more than one subunit in the filament [28]. An interaction of this kind would logically demand a more extended and spatially voluminous S2 interface than the small site described so far. Second, both in the S1 [12] and the S2 (severin) structure [14], the NH_2-terminal region and the long (actin binding) helix are spatially proximal, supporting a possible combined action of these two regions in the contact with the filament. In addition, such a proposed combined action of an NH_2-terminal and a COOH-terminal part in S2 would be similar to the one observed in S1. Residues Asp^{49} and Phe^{50} located in the S1 NH_2-terminus between β-strands 1 and 2 participate, together with residues from the α-helix (95–112), in forming a contact with actin [12].

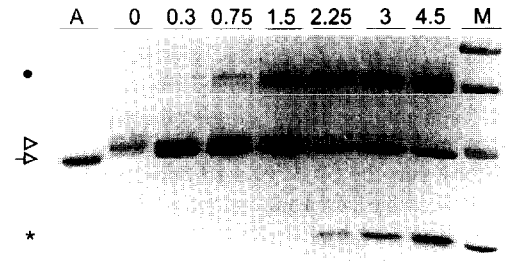

Fig. 4. Competitive binding of PS2 and gelsolin S2–3 to F-actin. SDS analysis of EDC crosslinking of 3 μM F-actin preincubated with 30 μM PS2 to which increasing concentrations of S2–3 (indicated above each lane in μM) were added. The lane headed 'A' contains actin without PS2. The non-crosslinked S2–3, non-crosslinked Sactin, the actin-PS2 and actin-S2–3 crosslink are indicated by an asterisk, an arrow, an arrowhead and a dot, respectively.

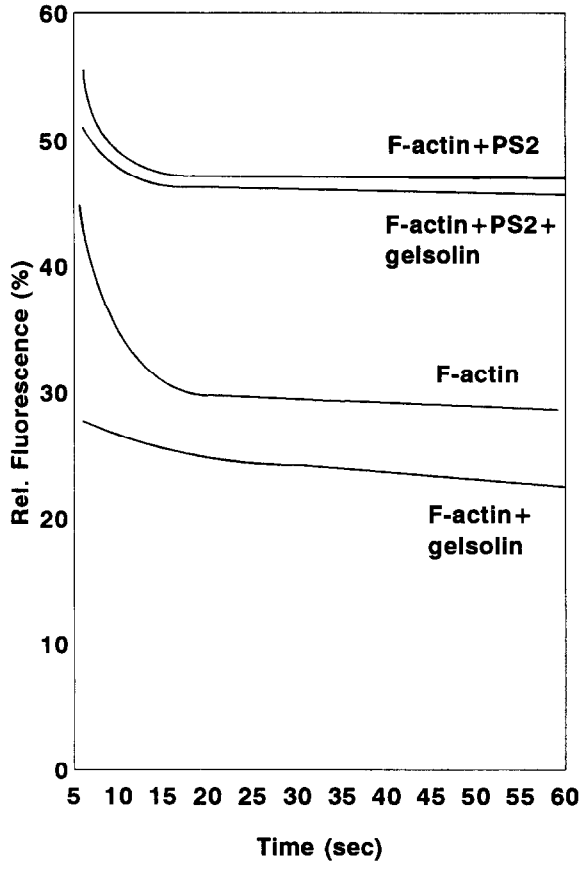

Fig. 5. We diluted F-actin, capped at the barbed end, and preincubated with PS2 in G-buffer in the presence (a) and absence (b) of gelsolin (0.4, 100 and 0.05 μM final concentrations of actin, PS2 and gelsolin). The same was done with omission of PS2 (c and d). The relative fluorescence is shown as a function of time, with measurements starting 30 s after dilution.

Sun et al. [16] reported that an NH_2-terminal deletion mutant of S2 containing residues 173–266, and thus also the PS2 sequence, no longer bound to F-actin. The loss in F-actin binding activity they observed can be due to the fact that residues 196–226 on their own bind with too low an affinity for complex formation to be detected in the assay used; however, more likely, as put forward by these authors themselves, it can be due to a changed conformation of this truncated S2 as their gel filtration analysis revealed that this mutant has a more elongated shape than the intact S2–3 and despite its smaller mass elutes earlier from the column.

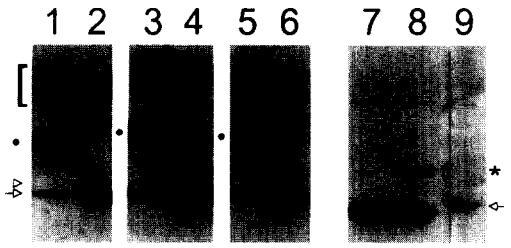

Fig. 6. Western blot analysis of the EDC crosslinking of actin alone (lane 7), actin and S2–3 (lanes 1, 3, 5), actin and PS2 (lanes 2, 4, 6) and actin and human profilin I (lanes 8, 9) using anti-actin specific antibodies against residues 228–257 (lanes 5, 6), 354–375 (lanes 3, 4, 9) and a monoclonal antibody specific for α-sarcomeric actin (lanes 1, 2, 7, 8). The positions of the non-crosslinked actin, the actin–PS2, the actin–S2–3 and the actin–profilin I crosslink are indicated by an arrow, an arrowhead, a dot and an asterisk, respectively.

The S2–F-actin binding sequence we newly identify here is located in the second half of segment 2 and is homologous to the actin binding site of segment 1 [12]. In S1, the central part of this sequence forms an α-helix that contributes to a large extent to the actin contact. Following the generally accepted view – which is strongly supported by the high structural similarity between S1 of gelsolin and S2 of severin [14] – that all segments in gelsolin adopt a same overall fold, the sequence we studied in S2 should also contain an α-helix. Our CD measurements indeed prove that the S2 peptide can adopt an α-helical conformation, albeit a very unstable one in aqueous solution at room temperature. However, as the corresponding S1 peptide (Fig. 1) reveals a similar low helical stability under the same conditions (Fig. 3), we may conclude that the PS2 sequence will be α-helical in the gelsolin protein.

In Fig. 7, we plotted PS2 on an α-helical wheel (starting from Ser^{202}) and compared it with the S1 actin binding helix. Most residues conserved between segments in the gelsolin family prove to be important in the internal packing of the domains in this case the packing of the α-helix onto the underlying β pleated sheet [29]. Fig. 7 shows these residues (shaded) for S1 and S2 of gelsolin and S2 of severin. The amino acids at the opposite side of the helix participate in actin binding, not only in S1 but, as shown here, also in S2. However, S1 and S2 bind to different sites on the actin filament because recombinant S1 and S2–3 can bind simulta-

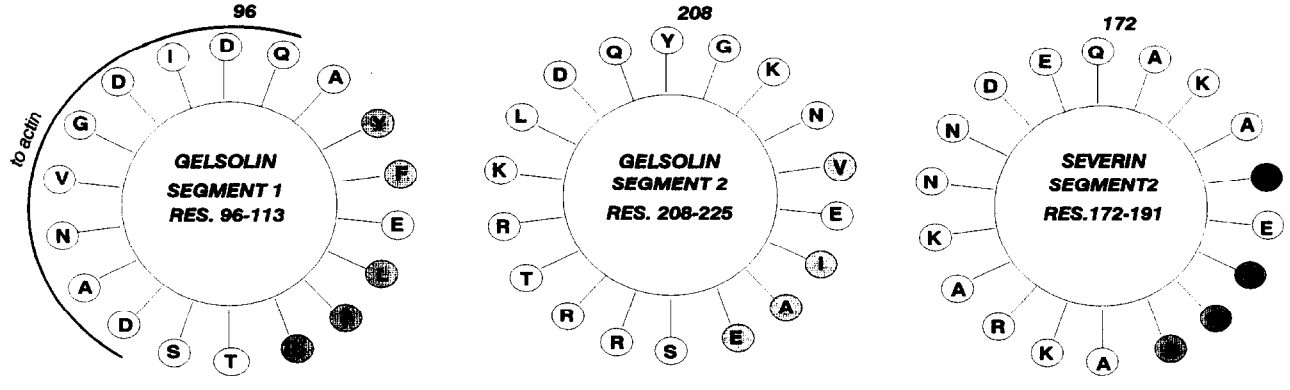

Fig. 7. Helical wheel presentation of the actin binding helices of gelsolin segments 1 and 2 and severin segment 2 [12,13]. Residues directed towards the gelsolin S1 and severin S2 core and the homologous residues in gelsolin S2 are shaded. The side of the gelsolin segment 1 helix known to face actin [12] is indicated.

neously to actin [8]. From the crystal structure it is clear that S1 binds between actin subdomains 1 and 3 [12]. From a mechanistic point of view, S2 is proposed to bind along the filament. MacGough and Way [30] modelled the α-actinin A1–2, which can functionally replace S2–3 [11], on F-actin and showed that contacts are made with subdomain 2 and subdomain 1 of two neighboring protomers along the longitudinal axis. Our immune data demonstrate that S2–3 and PS2 bind neither between actin residues 21–44 (the solvent exposed part of the epitope of the sarcomeric α-actin specific antibody) nor (unlike S1) near the COOH-terminus of actin. The latter again stresses the different target sites of S1 and S2 on actin. This distinction must arise from variation in the residues on the solvent exposed side of the actin binding helix in S1 and S2 as illustrated in Fig. 7. The hydrophobic character of S1 residues I^{103} and V^{106}, both essential in the contact with actin subdomain 1, is not conserved in S2 of gelsolin and related proteins. L^{212}, the only hydrophobic residue on the solvent exposed site of the S2 helix, is not present in the second domain of other gelsolin family members. However, the basic character of S2 residues 211, 213 and 222 is absolutely conserved throughout different S2 segments in both vertebrate and invertebrate species suggesting they are functionally relevant. The corresponding residues in S1 are acidic or uncharged. This indicates that although S1 and S2 are highly similar in overall structure, homologous surface regions of both segments (the solvent exposed residues in 95–112 [12] and 198–227 (this study)) have evolved to generate different actin binding properties. Thus, divergent evolution has produced a more powerful modulator of actin function.

In summary, this report contributes to understanding the complex mode of interaction of gelsolin and related proteins with actin filaments. Using a peptide mimetic, we identified extra residues of gelsolin involved in filament side-binding. As these are located in S2 at an analogous position as the actin binding helix of S1, the parallel between S1 and S2 that was already evident at the level of domain structure can be further extended. A positionally similar part of both segments is presented to actin, although the surface residues have evolved to fit the different actin target sites of S1 and S2.

Acknowledgements: We would like to thank Prof. Dr. Rossenu for use of the spectropolarimeter to perform the circular dichroism experiments and Mr. J. Van Damme for performing mass measurements. C.A. is a research associate of the Belgian National Fund for Scientific Research (N.F.W.O.). This work was supported by the Human Capital and Mobility Program of the European Community and Grant GOA-91/96-3 to J.V. and by EC Grant CI1-CT93-0049 and Grant 3.0008.94 of the FGWO to C.A.

References

[1] Kwiatkowski, D.J., Stossel, T.P., Orkin, S.H., Mole, J.E., Colten, H.R. and Yin, H.L. (1986) Nature 323, 455–458.
[2] Janmey, P.A. and Stossel, T.P. (1987) Nature 325, 362–364.
[3] Weeds, A. and Maciver, S. (1993) Curr. Opin. Cell Biol. 5, 63–69.
[4] Bryan, J. (1988) J. Cell Biol. 106, 1553–1562.
[5] Way, M., Gooch, J., Pope, B. and Weeds, A.G. (1989) J. Cell Biol. 109, 593–605.
[6] Kwiatkowski, D.J., Janmey, P.A. and Yin, H.L. (1989) J. Cell Biol. 108, 1717–1726.
[7] Pope, B., Maciver, S. and Weeds, A.G. (1995) Biochemistry 34, 1583–1588.
[8] Pope, B., Way, M. and Weeds, A.G. (1991) FEBS Lett. 280, 70–74.
[9] Yin, H.L., Iida, K. and Janmey, P.A. (1988) J. Cell Biol. 106, 805–812.
[10] Way, M., Pope, B. and Weeds, A.G. (1995) J. Cell Biol. 119, 835–842.
[11] Yu, F.-X., Zhou, D. and Yin, H.L. (1991) J. Biol. Chem. 266, 19269–19275.
[12] McLaughin P.J., Gooch, J.T., Mannherz, H.-G. and Weeds, A.G. (1993) Nature 364, 685–692.
[13] Schnuchel, A., Wiltscheck, R., Eichinger, L., Schleicher, M. and Holak, T. (1995) J. Mol. Biol. 247, 21–27.
[14] Markus, M.A., Nakayama, T., Matsudaira, P.T. and Wagner, G. (1994) Protein Sci. 3, 70–81.
[15] Eichinger, L., Noegel, A.A. and Schleicher, M. (1991) J. Cell Biol. 112, 665–676.
[16] Sun, H.Q., Wooten, D. Janmey, P.A. and Yin, H.L. (1994) J. Biol. Chem. 269, 9473–9479.
[17] de Arruda, M.V., Bazari, H., Wallek, M. and Matsudaira, P. (1992) J. Biol. Chem. 267, 13079–13085.
[18] Southwick, F. (1995) J. Biol. Chem. 270, 45–48.
[19] Spudich, J.A. and Watt, S. (1971) J. Biol. Chem. 246, 4866–4871.
[20] Kouyama, T. and Michashi, K. (1981) Eur. J. Biochem. 114, 33–38.
[21] Vancompernolle, K., Goethals, M., Huet, C., Louvard, D. and Vandekerckhove, J. (1992) EMBO J., 11, 4739–4746.
[22] Staros, J.V., Wright, R.W. and Suringle, D.M. (1986) Anal. Biochem. 156, 220–222.
[23] Mumby, S.M. and Gilman, A.G. (1991) Methods Enzymol. 195, 215–253.
[24] Towbin, H., Staehelin, T. and Gordon, J. (1979) Proc. Natl. Acad. Sci. USA 76, 4350–4354.
[25] Nelson, J.W. and Kallenbach, N.R. (1986) Proteins Struct. Funct. Genet. 1, 211–217.
[26] Schutt, C.E., Myslik, J., Rozycki, M.D., Gonnesekere, N.C.W. and Lindberg, U. (1993) Nature 365, 810–816.
[27] Vandekerckhove, J., Kaiser, D.A. and Pollard, T.D. (1989) J. Cell Biol. 109, 619–626.
[28] McGough, A. and Way, M. (1995) J. Struct. Biol. 115, 144–150.
[29] Ampe, C. and Vandekerckhove, J. (1994) Semin. Cell Biol. 5, 175–182.
[30] McGough, A., Way, M. and DeRosier, D. (1994) J. Cell Biol. 126, 433–443.